

# 000 001 002 003 004 005 006 007 008 009 010 011 012 013 014 015 016 017 018 019 020 021 022 023 024 025 026 027 028 029 030 031 032 033 034 035 036 037 038 039 040 041 042 043 044 045 046 047 048 049 050 051 052 053 DIAGONAL BATCHING UNLOCKS PARALLELISM IN RECURRENT MEMORY TRANSFORMERS FOR LONG CONTEXTS

006 **Anonymous authors**

007 Paper under double-blind review

## 011 ABSTRACT

013 Long-context inference with Transformers is constrained by quadratic attention  
014 and linear memory growth. Many linear-time alternatives require pretraining from  
015 scratch, whereas Recurrent Memory Transformers (RMTs) convert pretrained  
016 models into segment-recurrent variants via finetuning without modifying the original  
017 model architecture. However, their sequential memory updates underutilize GPUs.  
018 We show that RMT-style architectures with *layer-level* memory (PRMTs) (e.g.,  
019 ARMT) can be among the most latency-efficient linear approaches when scheduled  
020 properly. We introduce *Diagonal Batching*, a compute-reordering scheme that  
021 preserves exact recurrence while exposing inter-step parallelism by executing "di-  
022 agonals" concurrently with grouped layers. On LLaMA (1B/3B/8B) up to 131,072  
023 tokens on A100/H100, Diagonal Batching achieves up to 3.3 $\times$  lower latency than  
024 full-attention inference and 1.8 $\times$  over a sequential ARMT baseline, with *no cus-  
025 tom CUDA kernels*. With the right scheduling, PRMTs achieve linear scaling with  
026 context length and stand out as competitive, scalable architectures among linear  
027 recurrent models.

## 029 1 INTRODUCTION

031 Transformer-based language models have not only revolutionized natural language processing  
032 (NLP) (Vaswani et al., 2017; Devlin et al., 2019; Radford et al., 2019), but also catalyzed the  
033 development of intelligent agents that can solve complex, multi-step problems in various domains by  
034 scaling up to large language models (LLMs) (OpenAI, 2023; Reid et al., 2024; Dubey et al., 2024).  
035 However, these transformer-based models have quadratic time complexity and a linear memory  
036 footprint with respect to the length of the input sequence. Consequently, real-world applications are  
037 limited by the context window size of standard transformers that can fit within hardware constraints.

038 From an engineering perspective, numerous optimizations have been proposed to improve atten-  
039 tion efficiency and manage GPU memory more effectively. Optimized attention kernels, such as  
040 FlashAttention (Dao et al., 2022; Dao, 2024) and the xFormers library (Lefauze et al., 2022),  
041 focus on reducing memory access overhead and maximizing throughput. Memory-saving atten-  
042 tion modifications like Multi-Query Attention (MQA) (Shazeer, 2019), Grouped Query Attention  
043 (GQA) (Ainslie et al., 2023), and Multi-head Latent Attention (MLA) (Liu et al., 2024a) lower GPU  
044 RAM usage by sharing and optimizing KV-cache. For distributed long-context training, methods like  
045 Ring Attention (Liu et al., 2024b) and Microsoft DeepSpeed's Ulysses (Jacobs et al., 2023) partition  
046 sequence data across multiple devices to scale beyond single-GPU memory limits.

047 Along with these engineering optimizations, alternative architectures to the standard Transformer  
048 have been explored. Recently, state-space and linear recurrent models, such as S4 (Gu et al., 2021),  
049 RWKV (Peng et al., 2023), RetNet (Sun et al., 2023), and Mamba (Gu & Dao, 2023; Dao & Gu,  
050 2024) have replaced the softmax attention with alternative read-write operations. These models offer  
051 efficient parallel training, like transformers, and require constant memory during inference, like  
052 RNNs. However, these approaches often suffer from reduced memory capacity (Jelassi et al., 2024)  
053 and decreased accuracy in read-write operations (Rodkin et al., 2024). Furthermore, both state-space  
models and Transformers face theoretical limits, such as the  $TC^0$  complexity bound on the class of

054 functions computable in a single forward pass (Merrill et al., 2024; Strobl et al., 2024), constraining  
 055 their expressivity despite massive parallelism.  
 056

057 Memory-augmented models (Weston et al., 2015; Sukhbaatar et al., 2015), especially memory-  
 058 augmented transformers with segment-level recurrence (Dai et al., 2019; Rae et al., 2020; Bulatov  
 059 et al., 2022; Hutchins et al., 2022) offer an alternative approach by compressing history into fixed-  
 060 size memory states and propagating them across segments. In Recurrent Memory Transformers  
 061 (RMT) (Bulatov et al., 2022), special memory tokens carry state between segments, and each  
 062 Transformer block acts as a recurrent cell. This approach reduces inference complexity to linear  
 063 time and constant memory, supporting arbitrarily long contexts (Bulatov et al., 2024). However,  
 064 the recurrent nature of RMT makes it not fully parallelizable; all subsequent layers have recurrent  
 065 dependencies, and all segments must be processed sequentially.  
 066

067 Parallel Recurrent Memory Transformers (PRMTs) (Rodkin et al., 2024) are a broader class of  
 068 architectures in which each layer maintains its own memory state. PRMTs localize recurrence within  
 069 layers and eliminate all inter-layer memory flow. The Associative Recurrent Memory Transformer  
 070 (ARMT) (Rodkin et al., 2024) belongs to this family and demonstrates exceptional scalability. It  
 071 maintains high quality on sequences of up to 50 million tokens, which is far beyond the capacity of  
 072 RMT and Mamba (Rodkin et al., 2024; Kuratov et al., 2024). Models such as RWKV, Mamba, and  
 073 other linear-recurrent architectures can also be considered members of the PRMT family due to their  
 074 layer-level memory design.  
 075

076 PRMTs are asymptotically linear, yet they run sequentially over segments, which underutilizes GPUs  
 077 for single, long input requests. Naive micro-batching and pipelining are not helpful because they  
 078 require sophisticated batching over very long input sequences. This leads to unpredictable SLAs  
 079 and even higher latencies, due to the co-execution of many large-context requests at the same time.  
 080 Moreover, for pipelining, kernels operate on small inputs (segment sizes typically under 1024),  
 081 leading to small kernels that are unable to utilize the GPU without micro-batching.  
 082

083 In this work, we introduce *Diagonal Batching*, a scheduling scheme that unlocks inter-segment  
 084 parallelism in PRMTs inference without altering their exact recurrence. By reorganizing the 2D grid  
 085 of layer and segment computations into independent "diagonals", our method enables concurrent  
 086 execution of up to  $N_{\text{Layers}}$  operations per GPU kernel launch, eliminating the need to use com-  
 087 plex pipelining or micro-batching at all, which greatly simplifies the complexity of large context  
 088 deployments. Diagonal Batching fully encapsulates transformer block computations across segments,  
 089 thus *eliminating the layer- and segment-level synchronization barriers* present in previous RMT  
 090 implementations. Diagonal Batching does not require writing custom CUDA kernels to achieve  
 091 efficiency.  
 092

093 We implement Diagonal Batching in the ARMT framework and evaluate its performance on a LLaMA-  
 094 1B, 3B, and 8B models with sequence lengths up to 131,072 tokens on an NVIDIA A100/H100  
 095 GPUs. Our experiments demonstrate a  $3.3 \times$  speedup over standard full-attention inference and a  
 096  $1.8 \times$  improvement relative to a sequential ARMT baseline for 1B models. We show that RMT-style  
 097 architectures with layer-level memory (PRMTs), such as ARMT, are among the most latency-efficient  
 098 linear approaches for long-context inference when scheduled properly (via Diagonal Batching).  
 099

100 Our contributions are:  
 101

- 102 1. We identify execution *scheduling*, rather than algorithmic complexity, as the primary utilization  
 103 bottleneck for RMT-style linear recurrent models, especially on small and medium segment sizes.  
 104
- 105 2. We show that ARMT linear transformer become highly latency-efficient when scheduled right  
 106 with *Diagonal Batching*, a simple, kernel-agnostic grouping schedule that preserves exact recurrence  
 107 and exposes up to  $N_{\text{layers}}$  inter-step parallelism, yielding near-linear latency scaling without custom  
 108 kernels.  
 109
- 110 3. We empirically show that, ARMT with Diagonal Batching exhibits the best *latency scaling with*  
 111 *context length* among the linear-recurrent baselines we tested (Mamba, RWKV); on LLaMA-1B  
 112 at 131,072 tokens it achieves  $3.3 \times$  lower latency than full attention and  $1.8 \times$  over a sequential  
 113 ARMT baseline, with  $\approx 1\%$  relative logit drift, comparable to the drift observed between SDPA and  
 114 FlashAttention.  
 115

116

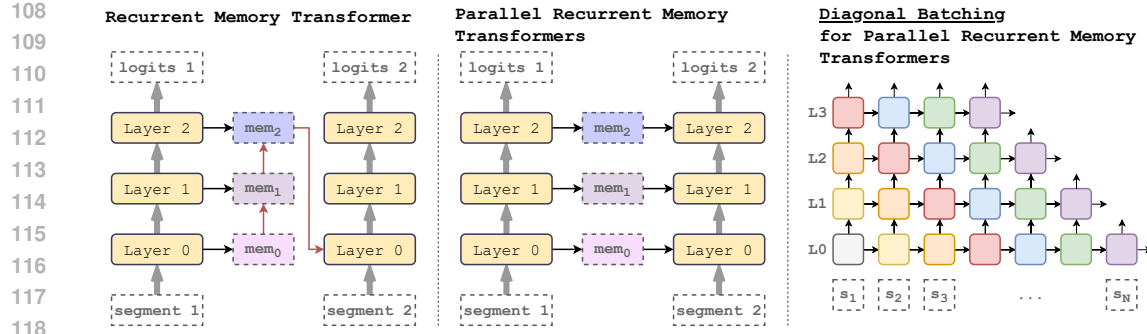


Figure 1: **Unlocking Parallelism in Recurrent Memory Transformers (RMT) with Diagonal Batching.** **Left:** RMT splits long sequences and processes segments sequentially. Each layer updates a memory (mem<sub>0</sub>, mem<sub>1</sub>, ...) and the final-layer memory is fed as input to the next segment; red arrows show the recurrent dependencies that force strictly sequential execution. **Center:** Parallel RMT (layer-level memory): each layer passes its own state to the same layer in the next segment, removing inter-layer dependencies but retaining per-layer segment recurrence. **Right:** Diagonal Batching rearranges the 2D grid of layers (rows) and segments (columns) into independent "diagonals" (same colored blocks). This allows all operations on one diagonal (up to N\_Layers) to execute concurrently on the GPU, thus eliminating the sequential bottleneck while preserving all layer-level recurrence.

## 2 BACKGROUND

### 2.1 RECURRENT MEMORY TRANSFORMERS

**Recurrent Memory Transformer (RMT)** extends standard Transformer architectures by introducing segment-level recurrence (Figure 1, left). Specifically, the hidden representations corresponding to a segment  $s$  are conditioned on a recurrent state  $M$ —referred to as the *memory*—propagated from the previous segment  $s - 1$ .

In the original RMT formulation, the memory state is implemented as a sequence of input embeddings. The memory update mechanism can be formally expressed as:

$$[_, _, M_s] = \text{Transformer}([M_{s-1}, H_{s-1}, M_{s-1}]), \quad (1)$$

where  $M_s$  denotes the memory state associated with segment  $s$ , and  $H_{s-1}$  represents the input embeddings from segment  $s - 1$ . The square brackets indicate concatenation of the input sequences.

**Associative Recurrent Memory Transformer (ARMT)** introduces a parallel memory mechanism designed to support a hierarchical memory structure. Unlike the original RMT, ARMT maintains distinct memory states across different layers. This design facilitates a more expressive memory representation by allowing each layer to store and update its own memory.

The memory update rule in ARMT is formulated as follows:

$$[_, M_s^l] = \text{TransformerLayer}(\text{AssociativeLayer}([H_{s-1}^{l-1}, M_s^{l-1}])) \quad (2)$$

$$k_i, v_i = W_K m_i, W_V m_i; \quad \beta_i = \sigma(W_\beta m_i); \quad A_0^l = \vec{0}; \quad z_0^l = \vec{0}; \quad (3)$$

$$\bar{v}_i = \frac{A_{s-1}^l \phi(k_i)}{(z_{s-1})^T \phi(k_i)}; \quad \gamma_i = 1 - \frac{(z_{s-1})^T \phi(k_i)}{\|\phi(k_i)\|^2}; \quad (4)$$

$$A_s^l = A_{s-1}^l + \sum_i \beta_i (v_i - \bar{v}_i) \otimes \phi(k_i); \quad z_s^l = z_{s-1}^l + \sum_i \gamma_i \phi(k_i). \quad (5)$$

$$\text{AssociativeLayer}(x_i) = \frac{A_{s-1}^l \phi(W_Q x_i)}{(z_{s-1}^l)^T \phi(W_Q x_i)}, \quad (6)$$

162 where  $m_i$  is the vector from  $M_s^l$ ,  $A_s^l \in \mathbb{R}^{d_{\text{model}} \times 6d_{\text{mem}}}$ ,  $z_s^l \in \mathbb{R}^{6d_{\text{mem}}}$ ,  $\phi$  is the untrained nonlinearity  
 163 DPFP-3 (Schlag et al., 2021),  $x_i$  is the vector from  $[H_{s-1}^{l-1}, M_s^{l-1}]$ .  
 164

165 This mechanism essentially implements quasi-linear attention with a delta rule for segment-level  
 166 recurrence.

167

## 168 2.2 LAYER-LEVEL RECURRENT MODELS

169

170 We call a model *layer-level recurrent* if, at time step  $t$  and layer  $\ell$ , the computation depends only  
 171 on  $(t, \ell - 1)$  and  $(t - 1, \ell)$  in the layer-time grid. The index  $t$  may denote either *tokens* or *segments*  
 172 (chunks of tokens). We use *Parallel Recurrent Memory Transformers* (PRMTs; Figure 1, center) as a  
 173 broad label for architectures that satisfy this dependency at either granularity. This class includes  
 174 ARMT (Rodkin et al., 2024), RWKV (Peng et al., 2023), Mamba (Gu & Dao, 2023; Dao & Gu,  
 175 2024), and other linear-recurrent models (Yang et al., 2024).

176 Per-layer memory enables scheduling policies that exploit parallelism across segments. *Diagonal*  
 177 *Batching* targets such layer-level recurrent architectures: it preserves the above dependency while  
 178 enabling parallel execution across segments. By contrast, RMT (Bulatov et al., 2022) introduces an  
 179 additional dependency on the previous step’s *final* layer; when the step is a segment  $s$ , output of  $(s, \ell)$   
 180 also depends on  $(s - 1, L)$  (Figure 1, left), which prevents diagonal scheduling.

181

## 182 2.3 EXISTING INFERENCE OPTIMIZATIONS TECHNIQUES FOR TRANSFORMER MODELS

183

184 Numerous techniques are proposed to speed up the inference of transformer models, including  
 185 FlashAttention (Dao et al., 2022; Dao, 2024), speculative decoding (Xia et al., 2023), quantiza-  
 186 tion (Frantar et al., 2022; Lin et al., 2024), among others. Practical methods should remain compatible  
 187 with these optimizations. Diagonal Batching is orthogonal to these methods and integrates with them  
 188 seamlessly, e.g., it can employ FlashAttention within segments computation and to compute attention  
 189 efficiently.

190

191 **Hardware utilization.** Effectiveness of individual operations is often analyzed via the roofline  
 192 model, which characterizes the performance limits of hardware based on computational intensity  
 193 and memory bandwidth (Williams et al., 2009). Transformer architecture mostly consists of matrix  
 194 multiplication - a compute bound operation. Matrix multiplication’s computational intensity does not  
 195 depend on batch size. However, the total achievable floating-point operations per second (FLOPS)  
 196 improves significantly, as larger batch sizes enable better parallel workload distribution across GPU  
 197 cores, optimizing hardware utilization (Dao et al., 2022).

198 Despite these benefits, a large batch size introduces significant memory demand. It mostly comes  
 199 from intermediate activation computations and storing output logits, which scales linearly with batch  
 200 size and sequence length. This limits practical usage of batching, as large language transformers  
 201 often use almost all available GPU memory.

202

## 203 3 DIAGONAL BATCHING METHOD

204

### 205 3.1 INTUITION AND DEPENDENCY GRAPH

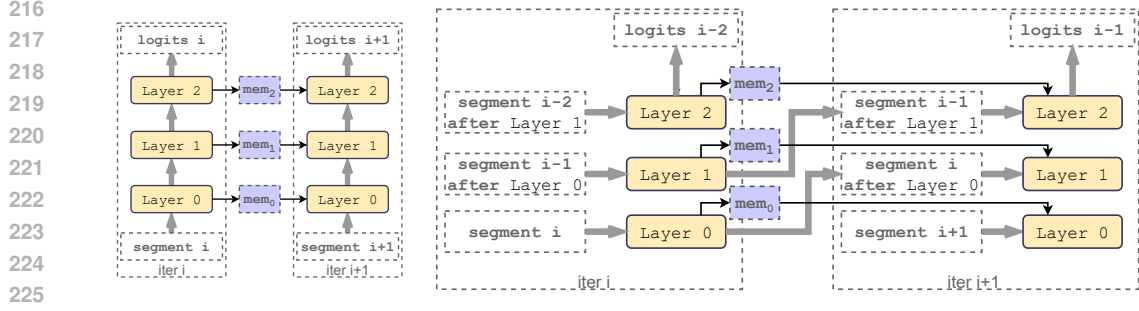
206 In the naive approach, we must perform many forward operations ( $n_{\text{segments}} \times n_{\text{layers}}$ )  
 207 using inputs of shape  $(\text{segment\_size}, \text{hidden\_size})$ . In PRMTs, each  $(\text{segment},$   
 208  $\text{layer})$  pair only depends on the preceding pairs:  $(\text{segment}, \text{layer-1})$  and  $(\text{segment-1},$   
 209  $\text{layer})$ .

210

211 Given this dependency, all pairs where  $\text{segment} + \text{layer} = i$  can be computed in parallel  
 212 during the  $i$ -th iteration. Each iteration can be visualized as a diagonal in the forward-pass computation  
 213 graph, as shown in Figure 1, right.

214

215 If the execution is not compute-bound, this diagonal execution approach can yield a significant  
 216 speedup for PRMT models.



(a) Baseline compute scheme. (b) Diagonal Batching: grouped compute scheme.

Figure 2: Baseline compute schedule in PRMTs leads to  $n_{\text{layers}} \times n_{\text{segments}}$  sequential operations. Diagonal Batching reduces this value to  $n_{\text{layers}} + n_{\text{segments}}$  by grouped computations.**Algorithm 1** GROUPED ARMT EXECUTION (DIAGONAL BATCHING)

---

**Require:** input sequence  $\mathcal{I}$ , number of layers  $L$ , grouped layer  $\mathcal{G}$

- 1: `ZEROGROUPEDMEMORY( $\mathcal{M}$ )`
- 2:  $segments \leftarrow \text{SEGMENT}(\mathcal{G}, \mathcal{I})$  ▷ token ids to segments with memory tokens
- 3:  $GInput \leftarrow []$ ,  $Out \leftarrow []$
- 4: **for**  $i = 0$  **to**  $L + |segments| - 1$  **do**
- 5:   **if**  $i < |segments|$  **then**
- 6:     prepend  $segments[i]$  to  $GInput$  ▷ ingest new segment
- 7:   **end if**
- 8:    $X \leftarrow \text{STACK}(GInput)$
- 9:   **if**  $i > 0$  **then**
- 10:      $X_{0:|X|-1} \leftarrow \text{ASSOCIATE}(\mathcal{G}, X_{0:|X|-1})$  ▷ memory association operation between consecutive segments
- 11:   **end if**
- 12:    $Y \leftarrow \text{GROUPEDFORWARD}(\mathcal{G}, X)$  ▷ multi-layer grouped call
- 13:    $\text{UPDATEMEM}(\mathcal{G}, Y, -\text{num\_mem\_tokens:})$  ▷ memory update for next segment
- 14:    $GInput \leftarrow \text{list of segments in } Y$
- 15:   **if**  $i \geq L - 1$  **then**
- 16:      $O \leftarrow GInput.\text{POPLAST}$  ▷ segment went through all layers
- 17:     append  $O$  to  $Out$
- 18:   **end if**
- 19: **end for**
- 20: **return** `CONCAT(Out)` ▷ final logits

---

## 3.2 BATCHING

Simplified description of the algorithm is given for ARMT in Algorithm 1. For other Parallel RMTs, the algorithm is the same, but without memory association and update operations.

**Lemma 3.1.** *Diagonal Batching completes the DAG in the minimum possible number of groups,  $N_{\text{segments}} + N_{\text{layers}} - 1$ , and schedules each node  $(i, j)$  in its earliest feasible group  $i + j$ .*

*Proof.* Topologically sort the DAG by the key  $(i, j)$  with root being  $(0, 0)$ . In this ordering, each node  $(i, j)$  appears at level  $i + j$ , which is therefore the earliest group it can occupy, and the longest path has length  $N_{\text{segment}} + N_{\text{layers}} - 1$  vertices. Hence, any schedule needs at least  $N_{\text{segment}} + N_{\text{layers}} - 1$  groups. Diagonal batching uses precisely those levels as its groups, achieving both bounds.  $\square$

## 3.3 IMPLEMENTATION DETAILS

To efficiently implement grouped layer computations, we modify the base model architecture. All layers are replaced with a single grouped layer, as shown in Figure 2. Using the initial layer of the model as the basis, we implement the following adjustments: (1) Replace the linear layers with a `GroupedMatmul` operation. The weights and biases are constructed by stacking those from the original layers. (2) Layer normalization weights are also replaced by stacking parameters across all

270 layers. Additionally, the forward pass is adapted to ensure correct broadcasting behavior. (3) All  
 271 other operations remain unchanged. However, they operate as though they handle significantly larger  
 272 batch sizes, contributing to parallel execution.

273 For the grouped matrix multiplication, we utilize the `GroupedGEMM` function from the CUTLASS  
 274 library with a minor optimization: the output tensor is pre-allocated as a single large tensor, which is  
 275 subsequently partitioned into individual submatrices without additional overhead.

276 **Difference from pipelining.** Diagonal Batching is a scheduling-and-layer-grouping method, not  
 277 pipeline parallelism. Unlike pipelines, it (1) uses a single control thread—no multi-thread/multi-  
 278 stream coordination or intrusive graph rewrites; (2) runs larger kernels instead of many small ones,  
 279 improving GPU utilization (see Figures 6 and 7) and avoiding CPU small-matrix special-casing (Yang  
 280 et al., 2021); and (3) requires no micro-batch overlap to hide bubbles as in pipelined systems (Huang  
 281 et al., 2019; Qi et al., 2023), yet achieves high utilization for single-request inference with a constant-  
 282 memory pattern, simplifying fleet deployment.

## 285 4 EXPERIMENTS

286 In the experiment section, we address two main questions regarding the Diagonal Batching method:  
 287 How much speedup we can get compared to the naive ARMT implementation in single request  
 288 inferences? How ARMT with Diagonal Batching scales compared to other linear recurrent models  
 289 (Mamba, RWKV) and to full-attention models (LLaMA)?

290 We start by showing that efficiency grows for individual bottleneck operations inside network - linear  
 291 layers and attention. Then, we show the resulting scaling for the transformer models with ARMT of  
 292 different sizes. We conducted all experiments with the models from the LLaMA-3 family (Grattafiori  
 293 et al., 2024).

### 294 4.1 INFERENCE SCALING

295 The performance increase for individual operations directly translates into overall model speedup.  
 296 We evaluate this effect on LLaMA ARMT models of varying sizes—160M (Table 9), 1B (Table 1),  
 297 3B (Table 7), and 8B (Table 8).

298 Across all model sizes and batch configurations, our implementation consistently achieves substantial  
 299 speedups over the default ARMT implementation. Gains are particularly pronounced for smaller  
 300 segment sizes. This is because, with larger matrix multiplications, hardware utilization is already  
 301 near peak FLOPS, leaving less room for group scaling.

302 A key implication of these results is that researchers can prioritize quality-driven choices for segment  
 303 size without being overly constrained by performance. Diagonal Batching decouples performance  
 304 from segment size, allowing better flexibility in architectural decisions.

### 305 4.2 SCALING BY MODEL FAMILY

306 We show how the different architecture families scale with input sequence length across different  
 307 model parameter sizes in Figure 3. Scaling for wider model classes includes measurement for  
 308 GPT and is shown in Appendix Figure 12. For model sizes under 0.5B, efficiency increase is very  
 309 significant, so the 3B model under Diagonal Batching performs similarly to the 0.4B model before  
 310 optimization. For bigger models, the gap is smaller, but allows to outperform the base non-linear  
 311 model starting from 32k context.

### 312 4.3 COMPARISON WITH OTHER LINEAR TRANSFORMERS

313 Comparison with other models shown in Figure 4. More extensive comparison shown in Ap-  
 314 pendix Figure 11 and Figure 10. Before our optimization, ARMT was slower on many configurations  
 315 than Mamba, RWKV, and sometimes even a quadratic-complexity transformer. With the Diagonal  
 316 Batching algorithm, ARMT outperforms other linear transformers with most configurations, provid-  
 317 ing a cost cut compared to non-linear transformers. For a fair comparison, we use the most efficient

324  
 325 Table 1: Diagonal Batching speeds up the execution for longer sequences — from  $1.1\times$  to  $2.7\times$   
 326 compared to base ARMT at 131072 sequence length. Execution time comparison (in seconds) and  
 327 relative speedups across different sequence lengths compared to LLama-3.2-1B-ARMT. Configuration  
 328 format: (segment\_size, memory\_tokens). Measured on Nvidia A100 GPU.

Method	Sequence Length					
	4096	8192	16384	32768	65536	131072
LLama-3.2-1B	0.024	0.026	0.376	0.926	2.460	8.160
<b>Configuration: (512, 128)</b>						
LLama-3.2-1B-ARMT	0.147	0.574	1.15	2.29	4.52	8.98
Diagonal Batching: LLama-3.2-1B-ARMT	0.283 <small>x0.52</small>	0.248 <small>x2.32</small>	0.454 <small>x2.53</small>	0.861 <small>x2.66</small>	1.67 <small>x2.71</small>	3.3 <small>x2.72</small>
<b>Configuration: (1024, 128)</b>						
LLama-3.2-1B-ARMT	0.149	0.291	0.578	1.15	2.3	4.48
Diagonal Batching: LLama-3.2-1B-ARMT	0.119 <small>x1.25</small>	0.196 <small>x1.49</small>	0.351 <small>x1.65</small>	0.656 <small>x1.75</small>	1.27 <small>x1.81</small>	2.48 <small>x1.81</small>
<b>Configuration: (2048, 128)</b>						
LLama-3.2-1B-ARMT	0.094	0.177	0.344	0.679	1.35	2.68
Diagonal Batching: LLama-3.2-1B-ARMT	0.108 <small>x0.87</small>	0.176 <small>x1.01</small>	0.304 <small>x1.13</small>	0.571 <small>x1.19</small>	1.11 <small>x1.22</small>	2.18 <small>x1.23</small>
<b>Configuration: (4096, 128)</b>						
LLama-3.2-1B-ARMT	0.082	0.155	0.301	0.594	1.18	2.35
Diagonal Batching: LLama-3.2-1B-ARMT	0.102 <small>x0.80</small>	0.172 <small>x0.90</small>	0.295 <small>x1.02</small>	0.553 <small>x1.07</small>	1.07 <small>x1.10</small>	2.1 <small>x1.12</small>

344  
 345 Table 2: Diagonal batching speeds up the execution - from 1.1 to 1.3 times comparing to base ARMT  
 346 for 131072 sequence length, LLama-3.2-3B-ARMT, measured on Nvidia A100 GPU.

Method	Sequence Length					
	4096	8192	16384	32768	65536	131072
LLama-3.2-3B	0.168	0.344	0.769	1.95	5.59	18.2
<b>Configuration: (1024, 128)</b>						
LLama-3.2-3B-ARMT	0.272	0.537	1.05	2.02	4.09	8.23
Diagonal Batching: LLama-3.1-3B-ARMT	0.274 <small>x0.99</small>	0.454 <small>x1.18</small>	0.833 <small>x1.26</small>	1.58 <small>x1.28</small>	3.1 <small>x1.32</small>	6.14 <small>x1.34</small>
<b>Configuration: (4096, 128)</b>						
LLama-3.2-3B-ARMT	0.203	0.39	0.765	1.52	3.01	6.01
Diagonal Batching: LLama-3.2-3B-ARMT	0.239 <small>x0.85</small>	0.411 <small>x0.95</small>	0.739 <small>x1.04</small>	1.4 <small>x1.09</small>	2.72 <small>x1.11</small>	5.37 <small>x1.12</small>

358 implementations for all architectures. Flash Attention 2 for non-linear transformers, ARMT and  
 359 ARMT with Diagonal Batching. We used mamba-ssm package for Mamba, and flash linear attention  
 360 for RWKV.

#### 363 4.4 DIAGONAL BATCHING VS MINI-BATCHING

364 Another way to increase compute load on GPUs is to increase the batch size. We evaluate the  
 365 effectiveness of Diagonal Batching compared to standard mini-batching by measuring compute time  
 366 per segment under identical hardware and model configurations. As shown in Figure 5, diagonal  
 367 batching achieves compute scaling per segment that closely matches micro-batching across almost all  
 368 tested scenarios.

369 To provide an upper bound on achievable performance, we also report the Ideal Even Load case,  
 370 where all segments are computed with a full grouped layer with maximum achievable FLOPS. One  
 371 can see that this even load setup is much better, mostly matching or overcoming the biggest batch  
 372 sizes. The gap between them is our current implementation inefficiency. Notably, Diagonal Batching  
 373 delivers substantial performance improvements for larger models (starting from 1B parameters),  
 374 particularly when segment sizes are moderate. For these configurations, Diagonal Batching matches  
 375 large batch sizes.

376 These findings suggest that Diagonal Batching effectively captures the utilization benefits of large-  
 377 batch inference — through parallelized scheduling rather than increased memory allocation.

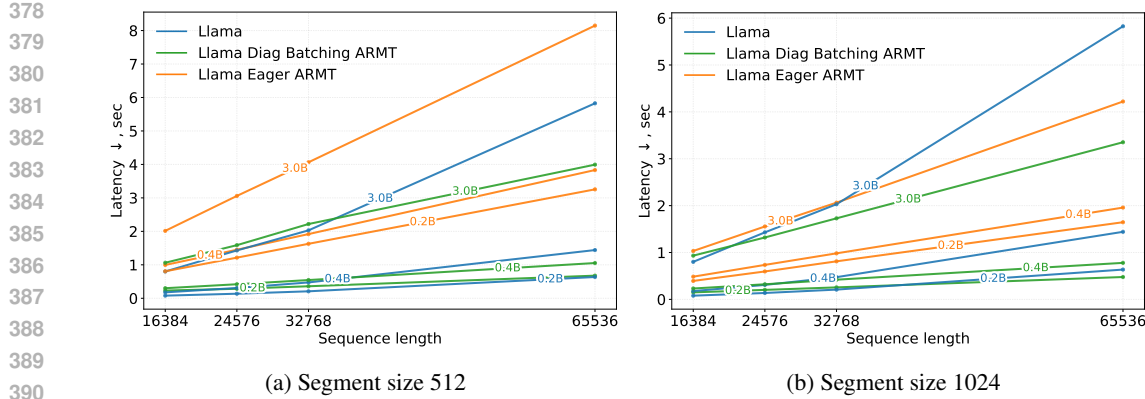


Figure 3: Diagonal batching lowers the scaling curve for the whole family of LLaMA models. For a 512 segment size, the 3B model with Diagonal Batching is performing almost as 0.4B with Eager implementation. Model’s family scaling for non-linear transformer, ARMT before and after Diagonal Batching usage. Measurements are done with bfloat16 on a single Nvidia A100 80Gb.

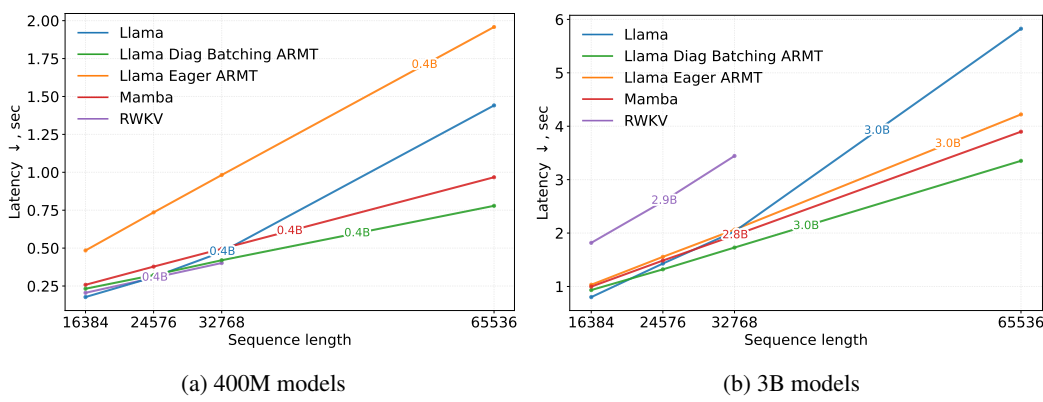


Figure 4: Diagonal batching makes ARMT the best performing linear architecture across different model sizes. Comparison between linear architectures and quadratic transformer grouped by the model’s sizes. Measured with bfloat16 on Nvidia A100.

#### 4.5 ERROR ACCUMULATION

We conducted an empirical investigation on computational error accumulation during the inference stage with Diagonal Batching. Our experiments show that the overall error is less than 2% for all sequences shorter than 32,768 tokens. This is comparable to other efficient layer implementations used in production. For example, we observed FlashAttention2 (Dao, 2024) gives 1-2% relative logits error compared to other attention implementations on the same input sequences.

The detailed error values for each segment are presented in Table 3. The error is calculated as the ratio of the Frobenius norm of the difference between the logits of the base ARMT implementation and the logits of ARMT with Diagonal Batching to the norm of the logits of the base ARMT. However, we find that effect of error accumulation on downstream tasks is negligible. To prove this, we evaluated the trained ARMT model both in original implementation and with Diagonal Batching; the results are presented in Table 4 in Appendix D. These results show that both implementations achieve the same results on the BABILong benchmark (Kuratov et al., 2024), while Table 5 in Appendix D shows that Diagonal Batching can increase the relative speed by up to 3.2x for 64k-length token sequences.

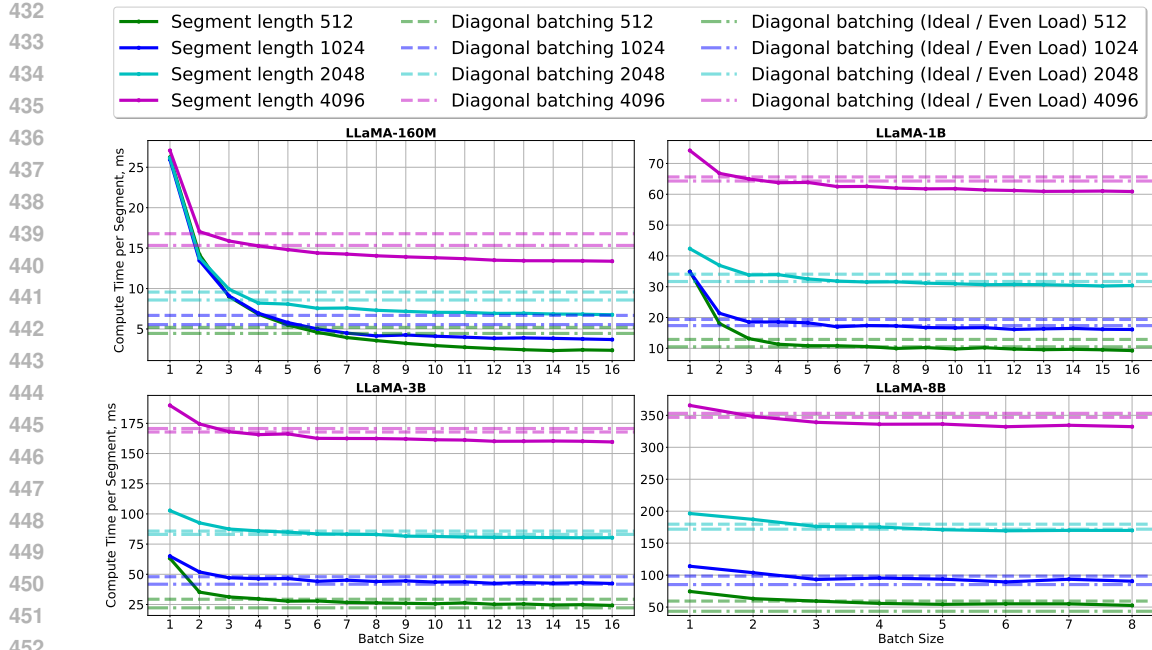


Figure 5: Ideal batch-size scaling vs grouped batching on Nvidia A100 for LLaMA models, time per segment in batch (group).

Table 3: During inference with diagonal batching, error accumulates but does not exceed 2%, which is comparable to the change of attention implementation (FlashAttention vs SDPA). The results for ARMT with Llama-3.2-1B-Instruct are shown with a segment size of 1024 tokens.

Number of segments	1	2	4	8	16	32	64	128
Diagonal Batching, Error, %	0.00	1.10	1.16	1.22	1.26	1.27	1.29	1.37
FlashAttention2 (Dao, 2024) vs torch SDPA, Error, %	1.25	1.15	1.17	1.22	1.36	1.45	1.79	2.04

## 5 CONCLUSIONS

We showed that the principal bottleneck in RMTs and their layer-memory variants (PRMTs) is not algorithmic complexity but *scheduling*: recurrent dependencies force fine-grained synchronization, which underutilizes modern accelerators. We introduced *Diagonal Batching*, a simple but powerful scheduling scheme that reorganizes the layer-segment computation grid into concurrency-friendly diagonals, enabling up to  $N_{\text{layers}}$  operations per kernel without altering exact recurrence. For single-request long-context inference (batch=1) on A100/H100, Diagonal Batching narrows the utilization gap without custom kernels, reducing cost per million tokens.

Relative to other linear-recurrent models, a base ARMT implementation is latency-inefficient. With Diagonal Batching, however, ARMT shows the *best latency scaling with context length*: latency grows near-linearly with length and matches or exceeds the end-to-end latency of custom-kernel baselines such as Mamba and RWKV at longer contexts. Compared to full-attention models, on LLaMA-1B at 131,072 tokens, ARMT with Diagonal Batching achieves  $3.3 \times$  lower latency than full-attention LLaMA-1B and  $1.8 \times$  over a sequential ARMT baseline, while preserving numerical fidelity on the same level as FlashAttention (about 1% relative logit error).

Considering these advantages, with right scheduling, Diagonal Batching turns theoretically appealing compute scaling of PRMTs into a practical solution for exact linear-time inference on extremely long contexts. By eliminating the major performance barrier, it positions memory-augmented recurrent Transformers as a competitive and scalable foundation for next-generation LLM applications that require efficient long-range input processing.

486 REPRODUCIBILITY STATEMENT  
487488 To ensure reproducibility of results, we are releasing the full codebase. Currently, the code can be  
489 found in the Supplementary Materials. Section C provides details on reproducibility, including used  
490 hardware, software, and models details.  
491492 REFERENCES  
493494 Joshua Ainslie, James Lee-Thorp, Michiel de Jong, Yury Zemlyanskiy, Federico Lebron, and Sumit  
495 Sanghai. Gqa: Training generalized multi-query transformer models from multi-head checkpoints.  
496 In *Proceedings of the 2023 Conference on Empirical Methods in Natural Language Processing*,  
497 pp. 4895–4901, 2023.498 Aydar Bulatov, Yury Kuratov, and Mikhail Burtsev. Recurrent memory transformer. *Advances in*  
499 *Neural Information Processing Systems*, 35:11079–11091, 2022.  
500501 Aydar Bulatov, Yuri Kuratov, Yermek Kapushev, and Mikhail Burtsev. Beyond attention: Breaking the  
502 limits of transformer context length with recurrent memory. *Proceedings of the AAAI Conference*  
503 *on Artificial Intelligence*, 38(16):17700–17708, Mar. 2024. doi: 10.1609/aaai.v38i16.29722. URL  
504 <https://ojs.aaai.org/index.php/AAAI/article/view/29722>.  
505506 Zihang Dai, Zhilin Yang, Yiming Yang, Jaime Carbonell, Quoc Le, and Ruslan Salakhutdinov.  
507 Transformer-XL: Attentive language models beyond a fixed-length context. In *Proceedings of the*  
508 *57th Annual Meeting of the Association for Computational Linguistics*, pp. 2978–2988, Florence,  
509 Italy, July 2019. Association for Computational Linguistics. doi: 10.18653/v1/P19-1285. URL  
510 <https://aclanthology.org/P19-1285>.511 Tri Dao. FlashAttention-2: Faster attention with better parallelism and work partitioning. In  
512 *International Conference on Learning Representations (ICLR)*, 2024.  
513514 Tri Dao and Albert Gu. Transformers are ssms: Generalized models and efficient algorithms through  
515 structured state space duality. In *International Conference on Machine Learning*, pp. 10041–10071.  
516 PMLR, 2024.517 Tri Dao, Daniel Y. Fu, Stefano Ermon, Atri Rudra, and Christopher Ré. FlashAttention: Fast and  
518 memory-efficient exact attention with IO-awareness. In *Advances in Neural Information Processing*  
519 *Systems (NeurIPS)*, 2022.520 Jacob Devlin, Ming-Wei Chang, Kenton Lee, and Kristina Toutanova. BERT: Pre-training of  
521 Deep Bidirectional Transformers for Language Understanding. In *Proceedings of the 2019*  
522 *Conference of the North American Chapter of the Association for Computational Linguistics: Human*  
523 *Language Technologies, Volume 1 (Long and Short Papers)*, pp. 4171–4186, 2019. URL  
524 <https://aclweb.org/anthology/papers/N/N19/N19-1423/>.  
525526 Abhimanyu Dubey, Abhinav Jauhri, Abhinav Pandey, Abhishek Kadian, Ahmad Al-Dahle, Aiesha  
527 Letman, Akhil Mathur, Alan Schelten, Amy Yang, Angela Fan, et al. The llama 3 herd of models.  
528 *arXiv preprint arXiv:2407.21783*, 2024.  
529530 Elias Frantar, Saleh Ashkboos, Torsten Hoefler, and Dan Alistarh. GPTQ: Accurate post-training  
531 compression for generative pretrained transformers. *arXiv preprint arXiv:2210.17323*, 2022.532 Aaron Grattafiori, Abhimanyu Dubey, Abhinav Jauhri, Abhinav Pandey, Abhishek Kadian, Ahmad  
533 Al-Dahle, Aiesha Letman, Akhil Mathur, Alan Schelten, Alex Vaughan, et al. The llama 3 herd of  
534 models. *arXiv preprint arXiv:2407.21783*, 2024.  
535536 Albert Gu and Tri Dao. Mamba: Linear-time sequence modeling with selective state spaces. *arXiv*  
537 *preprint arXiv:2312.00752*, 2023.  
538539 Albert Gu, Karan Goel, and Christopher Re. Efficiently modeling long sequences with structured  
state spaces. In *International Conference on Learning Representations*, 2021.

540 Yanping Huang, Youlong Cheng, Ankur Bapna, Orhan Firat, Dehao Chen, Mia Chen, HyoukJoong  
 541 Lee, Jiquan Ngiam, Quoc V Le, Yonghui Wu, et al. Gpipe: Efficient training of giant neural  
 542 networks using pipeline parallelism. *Advances in neural information processing systems*, 32, 2019.  
 543

544 DeLesley Hutchins, Imanol Schlag, Yuhuai Wu, Ethan Dyer, and Behnam Neyshabur. Block-recurrent  
 545 transformers. In Alice H. Oh, Alekh Agarwal, Danielle Belgrave, and Kyunghyun Cho (eds.),  
 546 *Advances in Neural Information Processing Systems*, 2022. URL <https://openreview.net/forum?id=uloenYmLCAO>.  
 547

548 Sam Ade Jacobs, Masahiro Tanaka, Chengming Zhang, Minjia Zhang, Shuaiwen Leon Song, Samyam  
 549 Rajbhandari, and Yuxiong He. Deepspeed ulysses: System optimizations for enabling training of  
 550 extreme long sequence transformer models. *arXiv preprint arXiv:2309.14509*, 2023.  
 551

552 Samy Jelassi, David Brandfonbrener, Sham M Kakade, and Eran Malach. Repeat after me: Trans-  
 553 formers are better than state space models at copying. In *International Conference on Machine  
 554 Learning*, pp. 21502–21521. PMLR, 2024.

555 Yuri Kuratov, Aydar Bulatov, Petr Anokhin, Ivan Rodkin, Dmitry Sorokin, Artyom Sorokin, and  
 556 Mikhail Burtsev. Babilong: Testing the limits of llms with long context reasoning-in-a-haystack.  
 557 In A. Globerson, L. Mackey, D. Belgrave, A. Fan, U. Paquet, J. Tomczak, and C. Zhang (eds.),  
 558 *Advances in Neural Information Processing Systems*, volume 37, pp. 106519–106554. Curran  
 559 Associates, Inc., 2024. URL [https://proceedings.neurips.cc/paper\\_files/paper/2024/file/c0d62e70dbc659cc9bd44cbcfc1cb652f-Paper-Datasets\\_and\\_Benchmarks\\_Track.pdf](https://proceedings.neurips.cc/paper_files/paper/2024/file/c0d62e70dbc659cc9bd44cbcfc1cb652f-Paper-Datasets_and_Benchmarks_Track.pdf).  
 560

561 Benjamin Lefauze, Francisco Massa, Diana Liskovich, Wenhan Xiong, Vittorio Caggiano, Sean  
 562 Naren, Min Xu, Jieru Hu, Marta Tintore, Susan Zhang, Patrick Labatut, Daniel Haziza, Luca  
 563 Wehrstedt, Jeremy Reizenstein, and Grigory Sizov. xformers: A modular and hackable transformer  
 564 modelling library. <https://github.com/facebookresearch/xformers>, 2022.  
 565

566 Ji Lin, Jiaming Tang, Haotian Tang, Shang Yang, Wei-Ming Chen, Wei-Chen Wang, Guangxuan  
 567 Xiao, Xingyu Dang, Chuang Gan, and Song Han. Awq: Activation-aware weight quantization for  
 568 on-device llm compression and acceleration. *Proceedings of Machine Learning and Systems*, 6:  
 569 87–100, 2024.  
 570

571 Aixin Liu, Bei Feng, Bin Wang, Bingxuan Wang, Bo Liu, Chenggang Zhao, Chengqi Dengr, Chong  
 572 Ruan, Damai Dai, Daya Guo, et al. Deepseek-v2: A strong, economical, and efficient mixture-of-  
 573 experts language model. *arXiv preprint arXiv:2405.04434*, 2024a.  
 574

575 Hao Liu, Matei Zaharia, and Pieter Abbeel. Ringattention with blockwise transformers for near-  
 576 infinite context. In *The Twelfth International Conference on Learning Representations*, 2024b.  
 577

578 William Merrill, Jackson Petty, and Ashish Sabharwal. The illusion of state in state-space models. In  
 579 *International Conference on Machine Learning*, pp. 35492–35506. PMLR, 2024.  
 580

581 OpenAI. Gpt-4 technical report, 2023.  
 582

583 Bo Peng, Eric Alcaide, Quentin Anthony, Alon Albalak, Samuel Arcadinho, Stella Biderman, Huanqi  
 584 Cao, Xin Cheng, Michael Chung, Leon Derczynski, Xingjian Du, Matteo Grella, Kranthi Gv,  
 585 Xuzheng He, Haowen Hou, Przemyslaw Kazienko, Jan Kocon, Jiaming Kong, Bartłomiej Koptyra,  
 586 Hayden Lau, Jiaju Lin, Krishna Sri Ipsit Mantri, Ferdinand Mom, Atsushi Saito, Guangyu Song,  
 587 Xiangru Tang, Johan Wind, Stanisław Woźniak, Zhenyuan Zhang, Qinghua Zhou, Jian Zhu, and  
 588 Rui-Jie Zhu. RWKV: Reinventing RNNs for the transformer era. In Houda Bouamor, Juan  
 589 Pino, and Kalika Bali (eds.), *Findings of the Association for Computational Linguistics: EMNLP  
 2023*, pp. 14048–14077, Singapore, December 2023. Association for Computational Linguistics.  
 doi: 10.18653/v1/2023.findings-emnlp.936. URL <https://aclanthology.org/2023.findings-emnlp.936/>.  
 590

591 Penghui Qi, Xinyi Wan, Guangxing Huang, and Min Lin. Zero bubble pipeline parallelism. *arXiv  
 592 preprint arXiv:2401.10241*, 2023.  
 593

594 Alec Radford, Jeff Wu, Rewon Child, David Luan, Dario Amodei, and Ilya Sutskever. Language  
 595 models are unsupervised multitask learners. 2019.

594 Jack W. Rae, Anna Potapenko, Siddhant M. Jayakumar, Chloe Hillier, and Timothy P. Lillicrap. Com-  
 595 pressive transformers for long-range sequence modelling. In *International Conference on Learning*  
 596 *Representations*, 2020. URL <https://openreview.net/forum?id=SylKikSYDH>.

597

598 Machel Reid, Nikolay Savinov, Denis Teplyashin, Dmitry Lepikhin, Timothy Lillicrap, Jean-baptiste  
 599 Alayrac, Radu Soricut, Angeliki Lazaridou, Orhan Firat, Julian Schrittweiser, et al. Gemini  
 600 1.5: Unlocking multimodal understanding across millions of tokens of context. *arXiv preprint*  
 601 *arXiv:2403.05530*, 2024.

602 Ivan Rodkin, Yuri Kuratov, Aydar Bulatov, and Mikhail Burtsev. Associative recurrent memory  
 603 transformer. *CoRR*, 2024.

604 Imanol Schlag, Kazuki Irie, and Jürgen Schmidhuber. Linear transformers are secretly fast weight  
 605 programmers, 2021. URL <https://arxiv.org/abs/2102.11174>.

606

607 Noam Shazeer. Fast transformer decoding: One write-head is all you need. *arXiv preprint*  
 608 *arXiv:1911.02150*, 2019.

609 Lena Strobl, William Merrill, Gail Weiss, David Chiang, and Dana Angluin. What formal languages  
 610 can transformers express? a survey. *Transactions of the Association for Computational Linguistics*,  
 611 12, 2024.

612 Sainbayar Sukhbaatar, Arthur Szlam, Jason Weston, and Rob Fergus. End-to-end memory networks,  
 613 2015.

614

615 Yutao Sun, Li Dong, Shaohan Huang, Shuming Ma, Yuqing Xia, Jilong Xue, Jianyong Wang, and  
 616 Furu Wei. Retentive network: A successor to transformer for large language models. *arXiv preprint*  
 617 *arXiv:2307.08621*, 2023.

618 Ashish Vaswani, Noam Shazeer, Niki Parmar, Jakob Uszkoreit, Llion Jones, Aidan N Gomez,  
 619 Łukasz Kaiser, and Illia Polosukhin. Attention is All you Need. In *Advances in neural informa-*  
 620 *tion processing systems*, pp. 5998–6008, 2017. URL <http://papers.nips.cc/paper/7181-attention-is-all-you-need>.

621

622 Jason Weston, Sumit Chopra, and Antoine Bordes. Memory networks. In Yoshua Bengio and Yann  
 623 LeCun (eds.), *3rd International Conference on Learning Representations, ICLR 2015, San Diego,*  
 624 *CA, USA, May 7-9, 2015, Conference Track Proceedings*, 2015. URL <http://arxiv.org/abs/1410.3916>.

625

626 Samuel Williams, Andrew Waterman, and David Patterson. Roofline: an insightful visual performance  
 627 model for multicore architectures. *Communications of the ACM*, 52(4):65–76, 2009.

628

629 Heming Xia, Tao Ge, Peiyi Wang, Si-Qing Chen, Furu Wei, and Zhifang Sui. Speculative decoding:  
 630 Exploiting speculative execution for accelerating seq2seq generation. In Houda Bouamor, Juan  
 631 Pino, and Kalika Bali (eds.), *Findings of the Association for Computational Linguistics: EMNLP*  
 632 2023, pp. 3909–3925, Singapore, December 2023. Association for Computational Linguistics.  
 633 doi: 10.18653/v1/2023.findings-emnlp.257. URL [https://aclanthology.org/2023.findings-emnlp.257/](https://aclanthology.org/2023.findings-emnlp.257).

634

635 Songlin Yang and Yu Zhang. Fla: A triton-based library for hardware-efficient implementations  
 636 of linear attention mechanism. January 2024. URL <https://github.com/fla-org/flash-linear-attention>.

637

638 Songlin Yang, Bailin Wang, Yu Zhang, Yikang Shen, and Yoon Kim. Parallelizing  
 639 linear transformers with the delta rule over sequence length. In *Advances in Neu-*  
 640 *ral Information Processing Systems 38: Annual Conference on Neural Information Pro-*  
 641 *cessing Systems 2024, NeurIPS 2024, Vancouver, BC, Canada, December 10 - 15,*  
 642 *2024*, 2024. URL [http://papers.nips.cc/paper\\_files/paper/2024/hash/d13a3eae72366e61dfdc7eea82eeb685-Abstract-Conference.html](http://papers.nips.cc/paper_files/paper/2024/hash/d13a3eae72366e61dfdc7eea82eeb685-Abstract-Conference.html).

643

644 Weiling Yang, Jianbin Fang, Dezun Dong, Xing Su, and Zheng Wang. Libshalom: Optimizing  
 645 small and irregular-shaped matrix multiplications on armv8 multi-cores. In *Proceedings of the*  
 646 *International Conference for High Performance Computing, Networking, Storage and Analysis*, pp.  
 647 1–14, 2021.

648 A THE USE OF LARGE LANGUAGE MODELS (LLMs)  
649650 LLMs were used exclusively for text polishing and editing (wording, spell checking).  
651652 B LIMITATIONS  
653654  
655 Despite its advantages, Diagonal Batching has several limitations. First, it is not directly compatible  
656 with the Recurrent Memory Transformers (RMTs) due to intra-layer recurrence. However, a more  
657 promising approach is to focus on Parallel RMTs, which have already been shown in previous works  
658 to be more effective (Rodkin et al., 2024). Second, our current implementation assumes a uniform  
659 layer configuration. When models employ heterogeneous layers or varied hidden sizes, applying the  
660 technique requires more intricate grouping logic and manual engineering. Finally, the achievable  
661 speedup increases with the number of layers. Therefore, shallower models or models with very few  
662 layers will only see modest performance gains.  
663664 C REPRODUCIBILITY  
665666 We attach an anonymized repository containing all inference/training code, experiment scripts,  
667 and figure notebooks. Experiments were run on a single NVIDIA A100 80 GB (and verified on  
668 H100) with PyTorch 2.5.1, CUDA 12.1, and BF16 precision. Exact package versions are pinned in  
669 requirements.txt in the artifact. Code can be found in Supplementary Materials.670 We evaluate LLaMA-3 and GPT ARMT variants with parameter sizes from approximate groups in  
671 200M, 400M, 1-2B, 3B. These groups follow publicly available checkpoints for GPT, LLaMA, and  
672 linear transformers (Mamba and RWKV). All ARMT checkpoints and conversion utilities follow the  
673 baseline repository instructions, which our artifact pins (commit hash is included in the README).  
674 Unless stated otherwise, we use the following parameters for experiments: single request (batch=1),  
675 segment sizes in 512, 1024, 2048, 4096, memory tokens = 16 for the main latency results and bfloat16.  
676 BABILong experiments use the task configs described by the benchmark authors.  
677678 To reproduce results for papers, see the attached repository:  
679680 1. ‘paper\_experiments/measure\_flops.ipynb’ - individual operation scaling  
681 2. ‘paper\_experiments/llamas\_batch\_scaling.ipynb’ - LLaMA scaling with batch size  
682 3. ‘paper\_experiments/ideal\_grouped\_scaling.ipynb’ - reproduce Ideal/Even Load baseline in  
683 paper  
684 4. ‘usage\_llama1b.ipynb’ - performance comparison of torch model, ARMT implementation,  
685 and grouped batching algorithm686 To reproduce the BABILong evaluation and training  
687688 1. Install additional dependencies - clone BABILong repo and prepare data:  
689 (a) ‘git clone https://github.com/booydar/babilong.git’  
690 (b) ‘unzip ./babilong/data/tasks\_1-20\_v1-2.zip’  
691 2. ‘run\_eval\_bl\_fast\_trained.py’ - example of evaluation on BABILong for ARMT and ARMT  
692 with Diagonal batching (trained on BABILong train set)  
693 3. ‘calc\_babilong\_scores.ipynb’ - extract and plot tables with BABILong scores and inference  
694 time for ARMT and ARMT with Diagonal batching  
695 4. ‘train\_babilong\_example.ipynb’ - example of finetuning ARMT with Diagonal batching on  
696 BABILong  
697 5. ‘run\_eval\_bl\_fast\_finetuned.py’ - example of evaluation on BABILong for ARMT with  
698 Diagonal batching after additional finetuning  
699700 Diagonal Batching benefits from base model kernel work optimizations, which are assumed to be  
701 presented (we use torch models from Huggingface Transformers); no custom CUDA is required.

702 Table 4: Diagonal Batching maintains the same scores as the original ARMT inference method on the  
 703 BABILong benchmark. Scores of the models were evaluated on the first two tasks: QA1 and QA2.  
 704

705 706 707 Task	708 Length, 709 tokens	710 711 712 713 714 LLama-3.2-1B 715 716 717 718 719 720 721 ARMT	710 711 712 713 714 715 716 717 718 719 720 721 LLama-3.2-1B 710 711 712 713 714 715 716 717 718 719 720 721 ARMT, 710 711 712 713 714 715 716 717 718 719 720 721 Diagonal Batching
710 711 712 713 714 715 716 717 QA1	0K	100	100
	1K	100	100
	2K	100	100
	4K	100	100
	8K	100	100
	16K	100	100
	32K	100	100
	64K	70	69
715 716 717 718 719 720 721 QA2	128K	4	4
	0K	100	100
	1K	100	100
	2K	100	100
	4K	100	100
	8K	99	100
	16K	98	98
	32K	94	94
722 723	64K	47	46
	128K	3	3

724 From grouped GEMM, we use CUTLASS GroupedGemm to avoid separate concatenation of input  
 725 segments (it is done implicitly by allocating the output blob as continuous memory).

726 We fix PyTorch/CUDA seeds and enable deterministic flags where possible; minor variance in end-  
 727 to-end latency is expected due to kernel autotuning and GPU clocks. Seeds and flags are set in the  
 728 provided scripts.

729 As a result, in the attachment are provided artifacts, including source code, pinned requirements,  
 730 ARMT patch + commit, run scripts, notebooks producing all plots/tables, and guidance commands  
 731 used for each result.

## 733 D EVALUATING MODELS WITH DIAGONAL BATCHING

736 Although diagonal Batching significantly speeds up the inference, it also introduces some numerical  
 737 drifts due to the optimized execution procedure. To estimate the effect of these drifts on practical  
 738 tasks, we evaluated the ARMT model on the BABILong benchmark Kuratov et al. (2024) with and  
 739 without diagonal Batching. The ARMT model was trained on the BABILong dataset with curriculum  
 740 learning on length up to 8192 tokens, similar to the approach described in Kuratov et al. (2024). After,  
 741 we evaluated this model with and without diagonal batching on QA1 and QA2 tasks from BABILong.  
 742 Note that we did not change the weights of the model in this experiment; we simply applied the  
 743 proposed Diagonal Batching grouping method.

744 The evaluation results are presented in Table 4. As one can see, despite the numerical drifts during  
 745 the forward pass, the generation results remain almost unchanged up to the 65536 input length. These  
 746 results show that diagonal batching preserves the quality of the generation of the trained ARMT  
 747 model and can be used as a drop-in replacement to speed up the inference.

748 We also compared the inference time of these two approaches on the same benchmark. In this  
 749 experiment, we measure not the forward pass time, but the generation time on the BABILong. Table 5  
 750 shows that the diagonal batching approach significantly speeds up the generation, up to 3 times on  
 751 the input length of 65536 tokens. During both of these experiments, we used the following ARMT  
 752 configuration - the size of the segment was set to 1024 tokens, the number of memory tokens was set  
 753 to 16, and the associative memory hidden size was 64.

754 Finally, we implemented the backward pass for diagonal batching to support training. Aligning  
 755 the training and inference code eliminates a discrepancy that is likely the source of logit-level  
 floating-point drift.

756  
757  
758  
759 Table 5: Diagonal Batching significantly speeds up ARMT inference on longer inputs. Inference time  
760 (in seconds) and relative speed-up of the models are given on the BABILong dataset, first two tasks.  
761  
762  
763  
764  
765  
766  
767  
768  
769

Task	Length, tokens	LLama-3.2-1B, ARMT	LLama-3.2-1B, ARMT, Diagonal Batching	Speed-up ( $\times$ times)
QA1	2K	13.43	15.06	0.89
	4K	22.45	17.99	1.25
	8K	41.41	22.49	1.84
	16K	79.16	33.12	2.39
	32K	153.68	54.20	2.84
	64K	302.15	94.36	3.20
QA2	2K	13.08	14.93	0.88
	4K	22.66	18.21	1.24
	8K	41.66	22.70	1.84
	16K	79.80	33.38	2.39
	32K	153.82	53.46	2.88
	64K	303.40	94.69	3.20

770  
771  
772 To further evaluate the difference between ARMT model with and without Diagonal Batching, we  
773 calculated how many tokens differ among tokens chosen by argmax during forward pass. The results  
774 are presented in Table 6.  
775

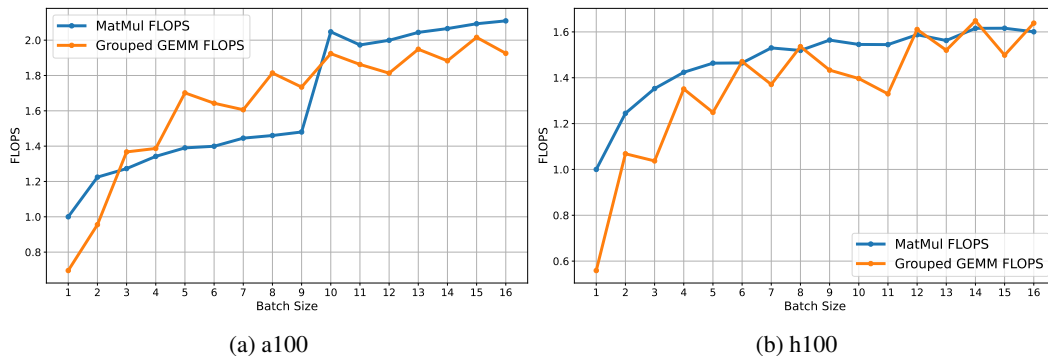
776 Table 6: During inference with diagonal batching, error accumulates in chosen by argmax tokens, but  
777 does not exceed 2%. The results for ARMT with Llama-3.2-1B-Instruct are shown with a segment  
778 size of 1024 tokens.  
779  
780

Number of segments	1	2	4	8	16	32	64	128
Diagonal Batching, percentage of different tokens chosen by argmax	0.00	0.05	0.02	0.05	0.09	0.12	0.12	0.13

## 784 D.1 LINEAR LAYER EFFICIENCY

785  
786 The only change from the base model is that we substitute linear layer with matrix multiplication  
787 to layers with grouped GEMM with the group size equal to all weights of the linear layers. In Figure 6  
788 we show that grouped GEMM FLOPS scales similarly through group size to GEMM with the  
789 corresponding batch size. This gives the basis that our method should scale similarly to the underlying  
790 model with batch size, as all other operations are basically the same (but in a different order).  
791

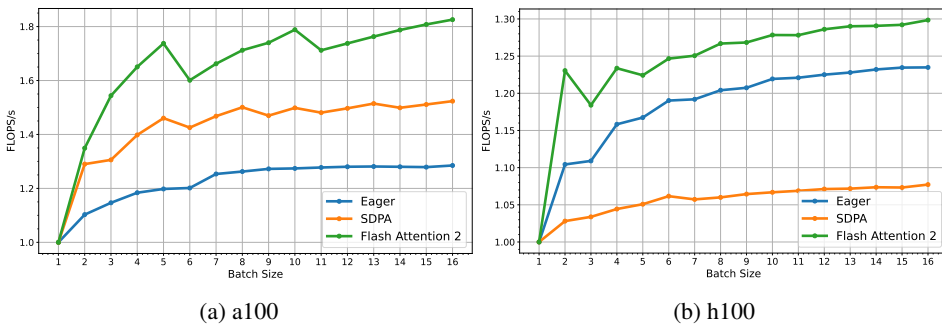
792 Second, we have a group size equal to the number of layers in the model. This way, we move the  
793 grouped GEMM operation to peak GEMM flops for a100 and h100 GPUs, ensuring high utilization.  
794 Corresponding FLOPS improvement shown in Figure 6.  
795



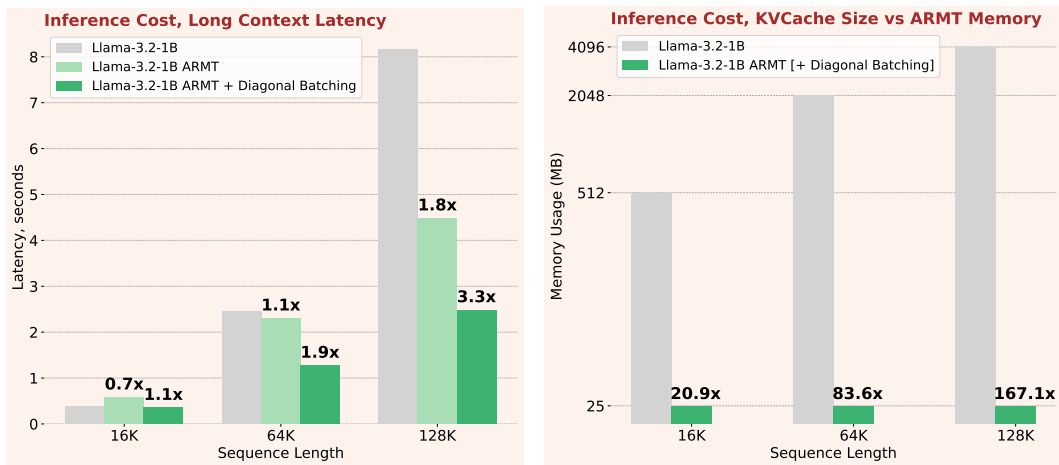
800 Figure 6: Cutlass Group GEMM scales similarly to batch size 1 Linear layer's matrix multiplication,  
801 starting from group size 4.  
802  
803  
804  
805  
806  
807  
808  
809

810  
811 D.2 ATTENTION LAYER EFFICIENCY

812 Our method does not modify the attention layer at all. Instead, attention just performs a batched  
813 operation with a batch size equal to the number of layers. This increases its performance to the  
814 implementation FLOPS peak. We show relative FLOPS speedups in Figure 7.



826  
827 Figure 7: Diagonal batching increases attention performance by treating groups as batches—similar  
828 to increasing the model’s overall batch size.  
829

830  
831 E ADDITIONAL MEASUREMENTS  
832

833  
834 Figure 8: **Diagonal Batching enables the Recurrent Memory Transformers (ARMT) to process**  
835 **128k token sequences 3.3x faster than the LLaMA-3.2-1B model, with 167.1x memory savings.**  
836 These results were obtained using an A100 GPU, and the segment size for the ARMT was set to  
837 1,024 tokens.

838 To clearly illustrate the speedup provided by the developed diagonal batching algorithm, we present  
839 relative improvements across various configurations and sequence lengths. Results for speedup  
840 against the original ARMT implementation are shown in Table 11 and against the underlying LLaMA  
841 model in Table 10. These measurements provide additional insights into how our method scales and  
842 compares to the baseline implementations.

843 We also present results for different size models of LLaMA-3 family Grattafiori et al. (2024):  
844 LLaMA-160M (Table 9), 1B (Table 1), 3B (Table 7), and 8B (Table 8) models.

Table 7: Diagonal batching speeds up the execution - from 1.1 to 1.3 times comparing to base ARMT for 131072 sequence length, LLama-3.2-3B-ARMT, measured on Nvidia A100 GPU.

Method	Sequence Length					
	4096	8192	16384	32768	65536	131072
Llama-3.2-3B	0.168	0.344	0.769	1.95	5.59	18.2
<b>Configuration: (1024, 128)</b>						
LLama-3.2-3B-ARMT	0.272	0.537	1.05	2.02	4.09	8.23
Diagonal Batching: LLama-3.1-3B-ARMT	0.274 <small>x0.99</small>	0.454 <small>x1.18</small>	0.833 <small>x1.26</small>	1.58 <small>x1.28</small>	3.1 <small>x1.32</small>	6.14 <small>x1.34</small>
<b>Configuration: (4096, 128)</b>						
LLama-3.2-3B-ARMT	0.203	0.39	0.765	1.52	3.01	6.01
Diagonal Batching: LLama-3.2-3B-ARMT	0.239 <small>x0.85</small>	0.411 <small>x0.95</small>	0.739 <small>x1.04</small>	1.4 <small>x1.09</small>	2.72 <small>x1.11</small>	5.37 <small>x1.12</small>

Table 8: Diagonal batching speed-ups the execution - from 1.05 to 1.14 times comparing to base ARMT for 131072 sequence length. Execution time comparison (in seconds) and relative speedups across different sequence lengths compared to LLama-3.2-8B-ARMT. Configuration in format (segment\_size, memory\_tokens). Nvidia A100 GPU.

Method	Sequence Length					
	4096	8192	16384	32768	65536	131072
Llama-3.1-8B	0.332	0.682	1.48	3.61	9.82	30.4
<b>Configuration: (1024, 128)</b>						
LLama-3.1-8B-ARMT	0.497	0.936	1.82	3.63	7.22	14.4
Diagonal Batching: LLama-3.1-8B-ARMT	0.478 x1.04	0.86 x1.09	1.64 x1.11	3.2 x1.13	6.34 x1.14	12.6 x1.14
<b>Configuration: (4096, 128)</b>						
LLama-3.1-8B-ARMT	0.384	0.754	1.48	2.95	5.86	11.7
Diagonal Batching: LLama-3.1-8B-ARMT	0.432 x0.89	0.781 x0.97	1.46 x1.01	2.83 x1.04	5.6 x1.05	11.1 x1.05

Table 10: Diagonal batching ARMT implementation allows to speedup the execution for longer sequences due to linear complexity - from 2.4 times to 3.8 times with respect to LLama-3.2-1B for 131072 sequence length. Table shows Diagonal Batching executor speedup against original LLama-3.2-1B for different methods across sequence lengths. Configuration in format (segment\_size, memory\_tokens). Measured on Nvidia A100 GPU.

Method	Sequence Length					
	4096	8192	16384	32768	65536	131072
LLama-3.2-1B, configuration: (512, 128)	0.085	0.105	0.828	1.075	1.473	2.473
LLama-3.2-1B, configuration: (1024, 128)	0.202	0.133	1.071	1.412	1.937	3.290
LLama-3.2-1B, configuration: (2048, 128)	0.222	0.148	1.237	1.622	2.216	3.743
LLama-3.2-1B, configuration: (4096, 128)	0.235	0.151	1.275	1.675	2.299	3.886

918  
 919 Table 9: Diagonal batching speed-ups the execution - from 1.6 to 3.9 times comparing to base ARMT  
 920 for 131072 sequence length. Execution time comparison (in seconds) and relative speedups across  
 921 different sequence lengths compared to LLama-160M-ARMT. Configuration in format (segment\_size,  
 922 memory\_tokens). Nvidia A100 GPU.

Method	Sequence Length					
	4096	8192	16384	32768	65536	131072
Llama-160M	0.017	0.033	0.075	0.196	0.594	2.03
<b>Configuration: (1024, 128)</b>						
LLama-160M-ARMT	0.105	0.211	0.422	0.877	1.72	3.37
Diagonal Batching: LLama-160M-ARMT	0.061 <small>x1.72</small>	0.087 <small>x2.43</small>	0.138 <small>x3.06</small>	0.243 <small>x3.61</small>	0.451 <small>x3.81</small>	0.855 <small>x3.94</small>
<b>Configuration: (4096, 128)</b>						
LLama-160M-ARMT	0.031	0.057	0.111	0.216	0.432	0.855
Diagonal Batching: LLama-160M-ARMT	0.046 <small>x0.67</small>	0.062 <small>x0.92</small>	0.094 <small>x1.18</small>	0.156 <small>x1.38</small>	0.284 <small>x1.52</small>	0.537 <small>x1.59</small>

931  
 932  
 933 Table 11: Diagonal batching allows to speedup the execution for longer sequences - from 1.1 times to  
 934 2.7 times with respect to base ARMT for 131072 sequence length. In cases when diagonal batching  
 935 is slower, we can fall back to the original inference algorithm at runtime. Table shows Diagonal  
 936 Batching executor speedup against original ARMT implementation for different methods across  
 937 sequence lengths. Configuration in format (segment\_size, memory\_tokens). Measured on Nvidia  
 938 A100 GPU.

Method	Sequence Length					
	4096	8192	16384	32768	65536	131072
LLama-3.2-1B, configuration: (512, 128)	0.519	2.315	2.533	2.660	2.707	2.721
LLama-3.2-1B, configuration: (1024, 128)	1.252	1.485	1.647	1.753	1.811	1.806
LLama-3.2-1B, configuration: (2048, 128)	0.870	1.006	1.132	1.189	1.216	1.229
LLama-3.2-1B, configuration: (4096, 128)	0.804	0.901	1.020	1.074	1.103	1.119

### E.1 APPLICATION TO OTHER MODELS

951  
 952 Diagonal Batching may also benefit other PRMT models as they contain recurrent structure. Examples  
 953 include Mamba and xLSTM. In these cases, diagonal batching can be applied with a segment size of  
 954 1, since these models exhibit token-level recurrence.

955 In Table 12 and Figure 9, we show that diagonal batching provides higher efficiency per segment by  
 956 increasing compute parallelism.

Method	Batch size							
	1	2	4	8	12	16	20	24
mamba_ssm with DB	<b>0.0000382</b>	<b>0.000038</b>						
mamba_ssm	0.00092	0.00046	0.00023	0.000115	0.000092	0.000059	0.000046	0.000039
No mamba_ssm with DB	<b>0.002865</b>	<b>0.002865</b>	<b>0.002865</b>	<b>0.002865</b>	<b>0.002865</b>	<b>0.002865</b>	<b>0.002865</b>	<b>0.002865</b>
No mamba_ssm	0.0658	0.03547	0.01778	0.00929	0.005743	0.00424	OOM	OOM

967 Table 12: Diagonal batching can be beneficial for Mamba on small batch sizes. Mamba throughput/  
 968 latency (in seconds) across batch sizes with and without efficient CUDA kernels for mamba  
 969 (*mamba\_ssm*). Measured on state-spaces/mamba-130m-hf model on single A100 inference. 8k  
 970 context used for measurements to prevent OOM on large batch sizes and, as mamba is token-recurrent  
 971 model, its efficiency does not increase when context is larger.

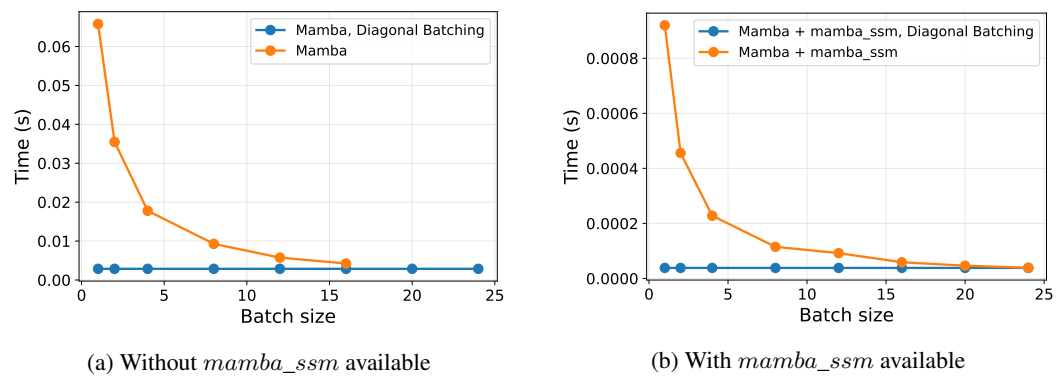


Figure 9: Comparison of Mamba performance with and without efficient CUDA kernels for mamba (*mamba\_ssm*).

To apply diagonal batching to Mamba in practice, one must rewrite the Mamba CUDA kernels to enable external segmentation of the forward pass, as the current implementation computes the full forward for each layer.

## E.2 ADDITIONAL COMPARISON WITH OTHER ARCHITECTURES

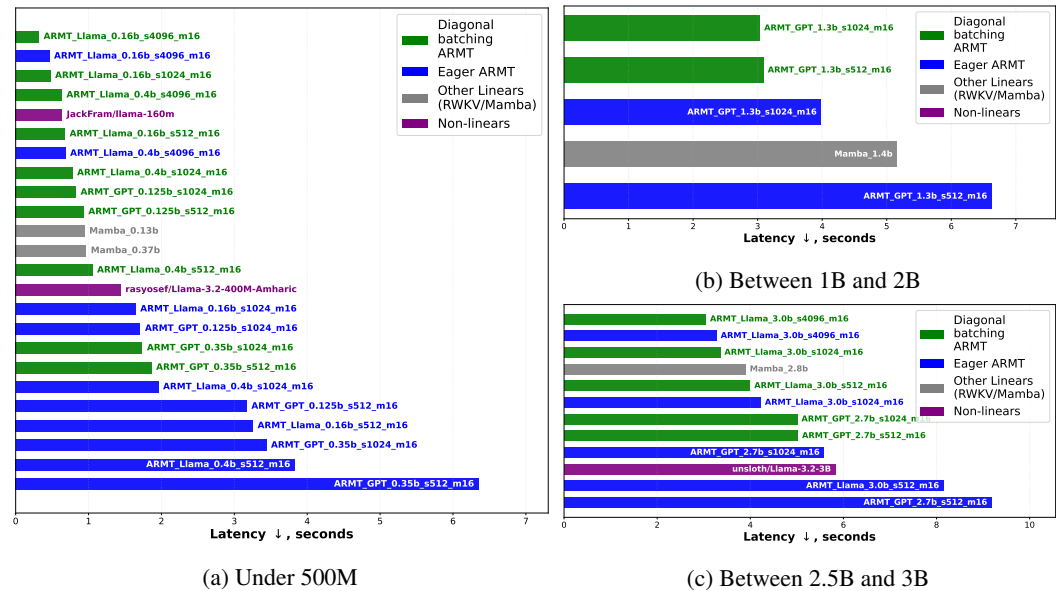


Figure 10: ARMT with Diagonal Batching is the best latency model in each category for the 64k context. ARMT+Diagonal Batching has very competitive performance across a wide variety of segment sizes. Comparison is made for open source models that can out of the box support such context. Reference efficient implementation is used - *mamba\_ssm* for Mamba and flash linear attention Yang & Zhang (2024) for RWKV. Single Nvidia A100 80Gb for measurements.

## E.3 DECODING STAGE WITH ARMT

Diagonal batching does not modify the decoding stage, meaning that ARMT inference with diagonal batching remains identical to the native ARMT implementation. However, ARMT provides several advantages over standard quadratic-time Transformers. Most importantly, it eliminates the need to store and repeatedly move large KV-caches between HBM and registers for each request - the cost that grows linearly with both load and context length. Instead, ARMT relies on compact associative

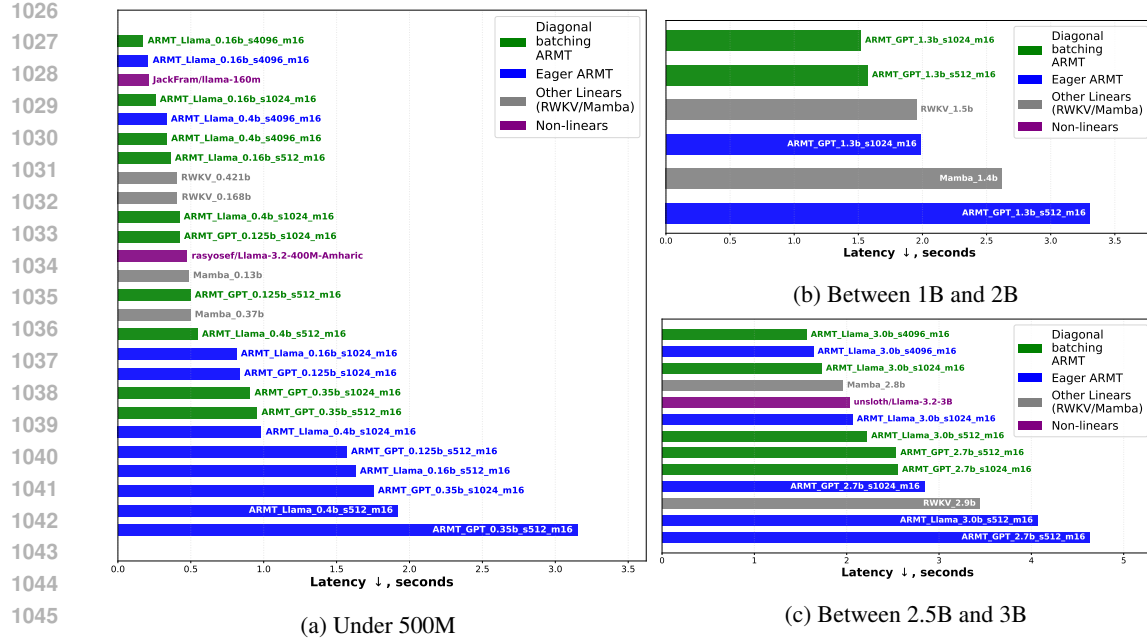


Figure 11: ARMT with Diagonal Batching is the best latency model in each category for the 32k context. ARMT+Diagonal Batching has very competitive performance across a wide variety of segment sizes. Comparison is made for open source models that can out of the box support such context. Reference efficient implementation is used - mamba-ssm for Mamba and flash linear attention for RWKV. Single Nvidia A100 80Gb for measurements.

memory produced during the prefill stage. This memory has fixed size per context and therefore scales only with the number of concurrent requests. As a result, ARMT can execute substantially more decoding phases in parallel within a disaggregated prefill–decode inference pipeline.

Table 13 shows that LLaMA-1B with ARMT sustains far more parallel requests before reaching OOM on an NVIDIA RTX 6000, and even very long contexts remain feasible.

Table 14 demonstrates that ARMT maintains stable decoding efficiency across large batch sizes, reducing memory-boundedness during decode. Further optimization of memory kernels for ARMT remains an open direction.

Context Length	Max Batch LLaMA	Max Batch LLaMA ARMT
4096	4	16
8192	1	16
16384	0	16
32768	0	16
65536	0	16

Table 13: ARMT allows to handle constant big batch size in parallel on decode, not depending on input context size. Maximum batch size before OOM on NVIDIA RTX 6000

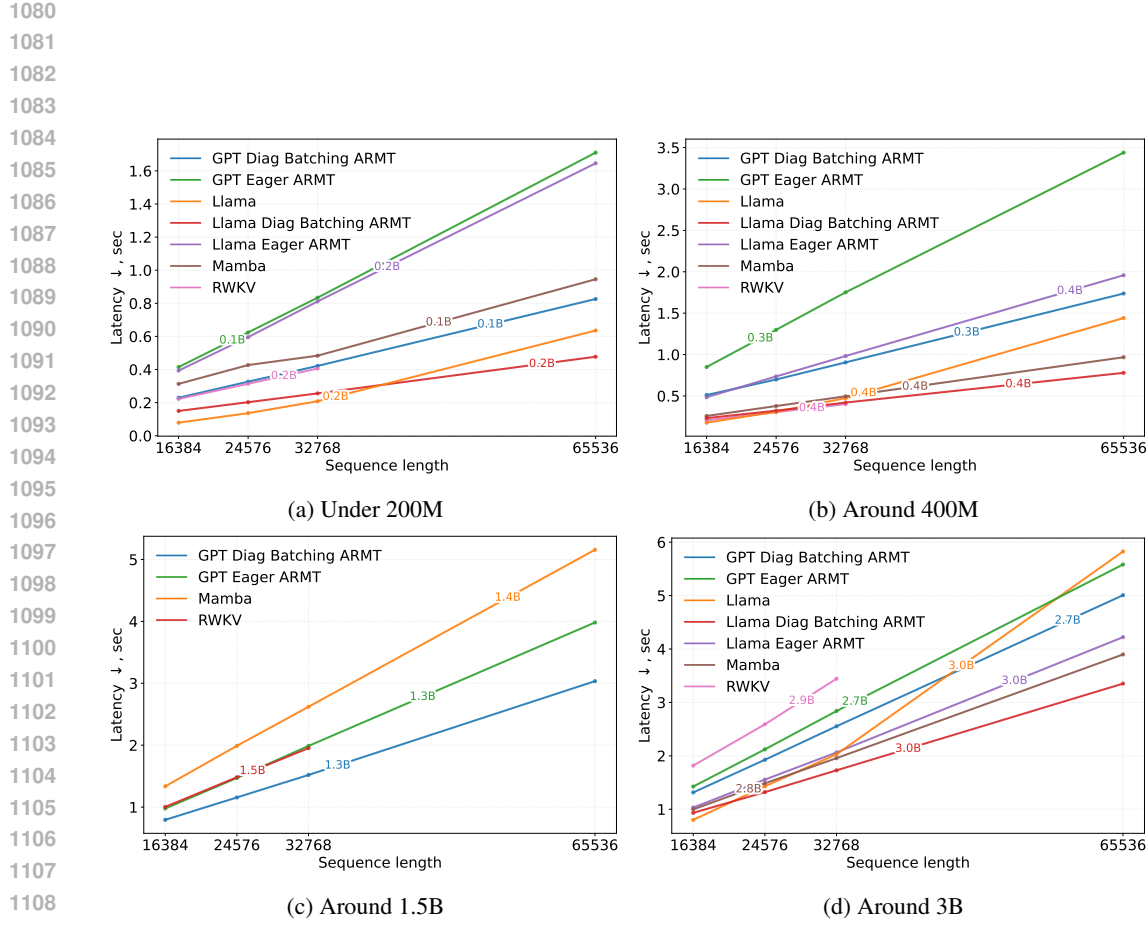


Figure 12: Plot comparison across different architectures grouped by model size.

Prefill Size	Decode 10 Tokens LLaMA, s	Decode 10 Tokens ARMT LLaMA, s
1024	0.007	0.025
4096	0.006	0.025
8192	0.007	0.081
16384	OOM	0.027
32768	OOM	0.026
65536	OOM	0.027

Table 14: Decode latency does not grow while batch size increase for ARMT model, yet it can handle much more requests in parallel than classic LLaMA transformer. Decode 10-token runtime comparison between LLaMA and ARMT-LLaMA for different prefill sizes. Measured on 48Gb NVIDIA RTX 6000.